Journal of Renewable Materials

Tech Science Press

DOI: 10.32604/jrm.2024.055492

ARTICLE

Green Chemistry of Cellulose Acetate Membrane Plasticized by Citric Acid and Succinonitrile for Lithium-Ion Battery Application

Christin Rina Ratri[1,2], Qolby Sabrina[2], Adam Febriyanto Nugraha[1], Sotya Astutiningsih[1] and Mochamad Chalid[1,*]

[1]Green Polymer Technology Laboratory, Department of Metallurgical and Materials Engineering, Faculty of Engineering, Universitas Indonesia, Depok, Jawa Barat, 16424, Indonesia

[2]Research Center for Advanced Materials, National Research and Innovation Agency, KST BJ Habibie Gd. 440-441, Tangerang Selatan, Banten, 15314, Indonesia

[*]Corresponding Author: Mochamad Chalid. Email: m.chalid@ui.ac.id

Received: 28 June 2024 Accepted: 19 September 2024 Published: 22 November 2024

ABSTRACT

Commercial lithium-ion batteries (LIBs) use polyolefins as separators. This has led to increased research on separators composed of renewable materials such as cellulose and its derivatives. In this study, the ionic conductivity of cellulose acetate (CA) polymer electrolyte membranes was enhanced via plasticization with citric acid and succinonitrile. The primary objective of this study was to evaluate the effectiveness of these plasticizers in improving cellulose-based separator membranes in LIBs. CA membranes were fabricated using solution casting technique and then plasticized with various concentrations of plasticizers. The structural, thermal, and electrochemical properties of the resulting membranes were characterized using Fourier Transform infrared (FTIR) spectroscopy, X-Ray Diffraction (XRD), Differential Scanning Calorimetry (DSC), Thermogravimetric Analysis (TGA), and Electrochemical Impedance Spectroscopy (EIS). The FTIR and XRD results confirmed the successful incorporation of citric acid and succinonitrile into the polymer matrix, while the TGA analysis demonstrated the enhanced thermal stability of the plasticized membranes. The shift in the glass transition temperature was determined by DSC analysis. Most notably, the EIS results revealed a significant increase in ionic conductivity, achieving a maximum of 2.7×10^{-5} S/cm at room temperature. This improvement was attributed to the effect of plasticizers, which facilitated the dissociation of lithium salts and increase the mobility of the lithium ions. The ionic conductivities of plasticized CA membranes are better than those of unmodified CA membranes and commercially available Celgard separator membranes: 4.7×10^{-6} and 2.1×10^{-7} S/cm, respectively. These findings suggest that citric acid and succinonitrile are effective plasticizers for cellulose acetate membranes, making them promising substitutes for commercial polyolefin separators in LIB applications.

KEYWORDS

Cellulose; polymer electrolyte; natural plasticizer; citric acid; succinonitrile

1 Introduction

The energy sector is a major concern in the context of global warming and climate change. It is crucial to reduce reliance on fossil fuels and to concentrate on improving sustainable energy generation and storage. As renewable energy sources become more widespread, there is a need for efficient energy storage systems to

store the electricity produced by these sustainable resources [1]. Addressing these challenges is essential for establishing a more sustainable and eco-friendly energy landscape in the coming years [2].

Lithium-ion batteries (LIBs) have emerged as pivotal energy storage devices, revolutionizing various technological applications. Lithium-ion batteries are distinguished from other common rechargeable batteries, such as Ni-Cd, Ni-MH, and lead-acid batteries, owing to their notable characteristics of high energy and power density, prolonged service life, and environmental friendliness. Consequently, they have been extensively used in consumer electronics. Their widespread utilization of portable electronics, electric vehicles, and renewable energy systems underscores their critical role in the advancement of contemporary energy storage technology [3]. A graphical scheme of the LIBs is shown in Fig. 1. Typically, a battery comprises of two electrodes, a separator membrane, and an electrolyte. During the charging process, Li ions moved from the cathode to the anode. In contrast, when a battery is in use and discharging, lithium ions are transferred from the anode to the cathode. LIBs can experience instability and generate excess heat when their internal temperature rises [4]. Separators within LIBs play a critical role in preventing short circuits and facilitating ion transfer [5].

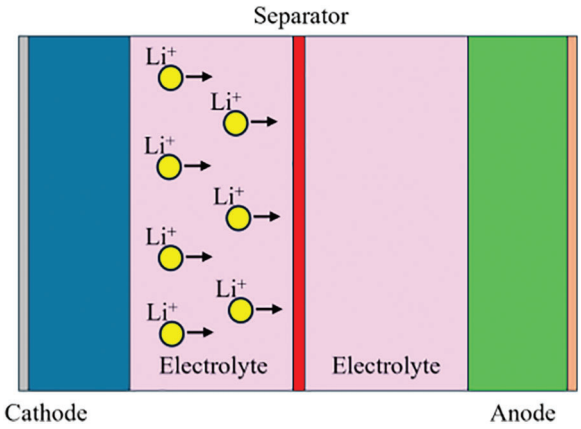

Figure 1: LIBs graphical scheme

Separators and electrolytes are essential components of the batteries. The separator serves the purpose of electrically isolating the two electrodes while also possessing porosity to facilitate the unrestricted movement of Li ions. On the other hand, the electrolyte allows efficient movement of Li+ ions between the electrodes. Ideally, a separator should be thin and porous, acting as both an electrical insulator and ionic conductor [6]. An ideal separator should facilitate rapid ion transfer, be easily wetted by liquid electrolytes to provide good contact, and withstand chemical reactions between electrodes and electrolytes. In mainstream batteries, the liquid electrolyte commonly features lithium hexafluorophosphate ($LiPF_6$) dissolved in carbonate solvents [7]. However, if the battery cells are heated above 70°C in an oxygen-deprived environment, the liquid electrolyte may break down, resulting in the generation of hydrocarbon gas. At temperatures as low as 50°C, electrolyte salts decompose, releasing hazardous gases such as pentafluorophosphate (PF_5) and hydrogen fluoride (HF). Notably, commercial separators, such as Celgard©, commence melting at 130°C, triggering the degradation of electrode materials and the release of oxygen [8].

In an attempt to promote green chemistry in renewable energy engineering, a substitute for the polyolefin Celgard separator has been pursued. One of them is cellulose, for which sources are abundant, and their intrinsic properties are promising. Bacterial cellulose has been proposed owing to its tunable porosity [9] and composite cellulose-based separator (CBS) because of its better cycling performance, which presents

a 356% longer lifetime compared to commercial Celgard [10]. Cellulose acetate is also a promising candidate, showing excellent thermal stability, as it can withstand heating up to 200°C [11].

Cellulose acetate is an environment-friendly material that can be used as a separator. It allows for easy porosity control and demonstrates favorable mechanical and thermal properties along with good hydrophilicity [12,13]. This investigation utilized dimethyl sulfoxide (DMSO), which is environmentally friendly, non-toxic, and has been proven to have superior efficacy compared to other solvents such as N-methyl pyrrolidone (NMP) [14,15].

The plasticization mechanism generally follows three main theories: lubricity theory, gel theory, and free volume theory. The lubricity theory by Kirkpatrick, Clark, and Houwink asserts that plasticizers work by lubricating polymer chains, where friction is reduced and macromolecular movement is promoted reciprocally. Gel theory, on the other hand, assumes that secondary forces in the polymer chains can be broken and intercalated by plasticizers by forming plasticizer-polymer bonds and shadowing macromolecule secondary bonds. Flexibility is promoted by plasticizer-free molecules acting as swelling agents [16]. Free volume theory was later added to the game by justifying the decrease in the glass transition temperature of the polymer. The free volume can be increased by increasing the number of end groups and/or side chains, adding low-molecular-weight compounds, and increasing the temperature [17]. In the separator/electrolyte system, increased free volume helps plasticize the polymer complex, thereby allowing global movement of lithium ions between electrodes. Various plasticizers have been used to improve the electrical performance of polymer electrolytes, such as glycerol in hydroxyethylcellulose (HEC)–lithium tetraborate ($Li_2B_4O_7$) complexes, dimethyl carbonate (DMC) in methyl cellulose (MC)–potassium hydroxide (KOH) complexes, propylene (PC), and ethylene carbonate (EC) in poly (methyl methacrylate) (PMMA)–lithium perchlorate ($LiClO_4$) complexes [18–20].

Succinonitrile is commonly used as a natural plasticizer to increase the ionic conductivity of composite polymer electrolytes (CPEs). Glutamic acid and glutamine are examples of succinonitrile precursors [21]. The inclusion of the ‘trans’ isomer impurity stabilizes the plastic crystal phase of succinonitrile, contributing to its improved performance [22]. Plastic crystals exhibit structural disorder, leading to increased plasticity and enhanced diffusivities compared with conventional rigid crystals [23]. Succinonitrile plastic crystal electrolytes demonstrate outstanding properties, including affordability, high room-temperature ionic conductivity of 10^{-3} S/cm, and a broad electrochemical window (>5 V *vs*. Li^+/Li) [24–26]. Succinonitrile retains a plastic crystalline phase within the temperature range of the transition temperature (−40°C) to the melting temperature (60°C). This characteristic enables it to remain in a solid state, ensuring high safety levels at room temperature [22]. Research by Wang et al. revealed that succinonitrile addition improved the ionic conductivity of a poly (ethylene oxide)–lithium bis (trifluoromethanesulfonyl) imide (LiTFSI) complex up to 2.85×10^{-4} S/cm [27].

Citric acid is a natural, organic acid extracted from fermented citrus fruits. It is biocompatible and has a multifunctional chemistry. It has a chemical formula of $C_6H_8O_7$, molecular weight of 210.14 g/mol, and acid dissociation constants (pKa) of 3.4, 4.7, and 6.4 [28]. Citric acid has been used as a cross-linking agent for cellulose. Citric acid is a more promising than other crosslinking agents because it comes from renewable ingredients, making it more environmentally friendly compared to its counterparts [29]. Citric acid forms cyclic anhydrides at elevated temperatures and esterifies the hydroxyl groups in the adjacent polymer chains.

This study focuses on the effect of using succinonitrile and citric acid as plasticizers for producing cellulose-based polymer electrolyte membranes. Both additives were used with various variations to analyze the effects of the amount and then compared to the unmodified and commercial Celgard membranes. Succinonitrile and citric acid additives are expected to have plasticizing effects on CA membranes as polymer electrolytes. In addition to improving ionic conductivity, the use of cellulose-

based materials as the polymer host, succinonitrile and citric acid as plasticizers, and DMSO as the solvent would be beneficial for the development of sustainable membrane fabrication in energy applications.

2 Materials and Methods

The membrane separator was fabricated by dissolving 7% w/v cellulose acetate (CA, Sigma Aldrich, Saint Louis, MO, USA, average Mn 30 kDa by GPC) in dimethyl sulfoxide (DMSO, Mercks). Additionally, electrolyte salt $LiClO_4$ (Merck), succinonitrile (Sigma Aldrich) and citric acid monohydrate (Merck) were incorporated with various variations as outlined in Table 1, illustrating the diverse combinations of additives used in the procedure. A commercial separator membrane (Celgard 2325, KGC Scientific, Shah Alam, Malaysia) was used throughout the experiment, without any pre-treatment.

Table 1: Sample designation and additive variations

Sample code	CA (gr)	$LiClO_4$ (gr)	Citric acid (gr)	Succinonitrile (gr)
CA	0.7	0	0	0
CA10	0.7	0.14	0	0
CASN0	0.7	0	0.028	0
CASN2	0.7	0.14	0.028	0
CASN4	0.7	0.14	0.056	0
CASN6	0.7	0.14	0.112	0
CAC0	0.7	0	0	0.028
CAC2	0.7	0.14	0	0.028
CAC4	0.7	0.14	0	0.056
CAC6	0.7	0.14	0	0.112

The mixture was stirred continuously on a hot plate at 100°C for 30 min until a smooth solution was formed. Subsequently, the cellulose acetate solution was poured into a petri dish. Solvent evaporation was performed in a vacuum oven. Initially, the samples were heated to 80°C for the first hour, and then the temperature was reduced to 60°C. Each sample was heated for 72 h for complete solvent removal. Following evaporation, the samples were left at room temperature until they detached from the petri dish.

The surface chemistry was observed using Fourier Transform infrared spectroscopy (FT-IR, Thermo Fisher Scientific, Nicolet iS10, Waltham, MA, USA). The spectra were recorded in the wavenumber range of 400–4000 cm^{-1}. Membrane crystallinity was investigated using X-Ray Diffractometer (XRD, Rigaku Smartlab, Tokyo, Japan) working on CuKα radiation at a scanning rate of 5°/min over 2θ range of 10°–60°. Surface and cross-sectional analyses were performed using a scanning electron microscope (SEM, Hitachi SU3500, Tokyo, Japan) at an acceleration voltage of 10 kV. The cross-sectional morphology was obtained using the freeze-fracture technique in liquid N_2. Thermogravimetric analysis (TGA) and Differential Scanning Calorimetry (DSC) were performed to observe the glass transition temperature and thermal stability under an inert atmosphere (N_2) at a heating rate of 10°C/min from 20°C to 500°C (TGA) and −20°C to 250°C (DSC).

Ionic conductivity measurements were performed using Electrochemical Impedance Spectroscopy (EIS, Autolab Potentiostat). The membrane was sandwiched between two stainless steels and crimped into a CR2032 battery coin cell. EIS measurements were performed by sweeping a constant voltage across a frequency range of 0.1 Hz–50 kHz at room temperature.

The ionic conductivity σ (S/cm) was calculated using Eq. (1):

$$\sigma = t/(R_b \times A), \quad (1)$$

where A is the contact area of the polymer electrolyte membrane (cm^2), t is the membrane thickness (cm), and R_b is the bulk resistance obtained from the intercept of the real impedance axis (Ω).

The electrochemical stability windows were established by linear sweep voltammetry (LSV) using a Wonatech Battery Cycler System. Plasticized membranes with the highest conductivity were sandwiched between stainless steels and subjected to a working voltage of 0–5.5 V, which is the typical operational voltage range for LIBs.

3 Results and Discussion

The FTIR spectra of the pristine CA membrane (CA) and plasticized CA membrane with citric acid (CAC) and succinonitrile (CASN), can be observed in Fig. 2. Notably, the distinct peak at 1740 cm^{-1}, which corresponds to stretching of the ester carbonyl group [30]. The shift to a higher energy of 1740 cm^{-1} rather than 1720 cm^{-1}, is likely attributed to the enhanced double bond character of the ester C=O group compared to that of a typical ketone group.

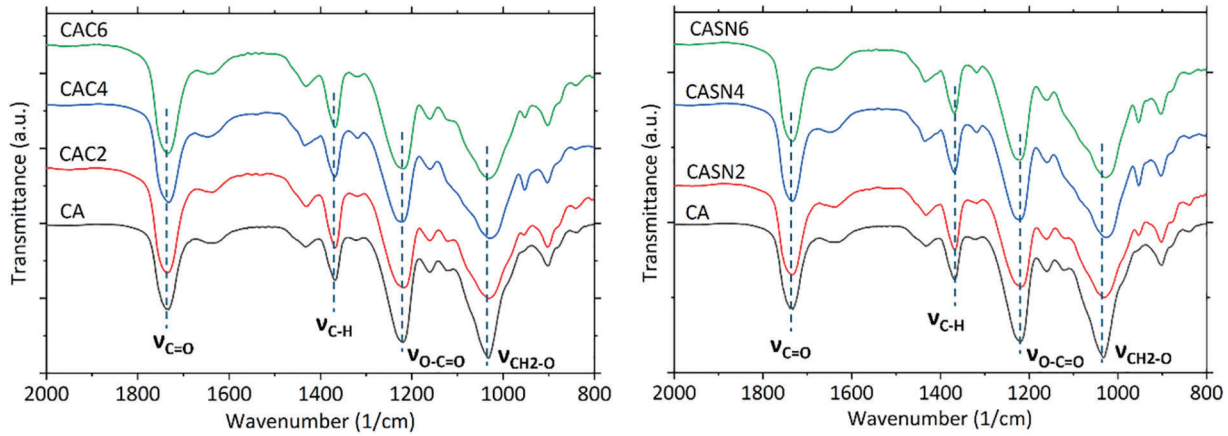

Figure 2: FTIR spectra of pristine and modified CA membrane

The presence of an O atom induces electron withdrawal, which results in the accumulation of electrons at this location. This leads to the development of a double bond character and necessitates a higher energy for bond excitation, as evidenced by the leftward shift [31]. Furthermore, the ester bond is supported by the presence of two distinct peaks in the OH group stretching. One peak was observed at 1050 cm^{-1}, representing a single CH_2-O bond, whereas the other peak appeared at 1230 cm^{-1}, corresponding to the O-C=O bond. The increase in energy observed later can be attributed to the same effect as that described for the ester carbonyl.

An absorption peak at 1159 cm^{-1} is observed, which could be attributed to the stretching of the ether bonds. This peak corresponded to both external (polymer bonds) and internal (cyclic bonds) stretching vibrations. The tertiary alcohol of citric acid was observed at 1110 cm^{-1}, while the other peak at 1159 cm^{-1} is attributed to ether bonds. There is a notable peak that spans from 3300 to 3500 cm^{-1}; this peak corresponds to the stretching of OH groups and coincides with the peak of aliphatic C-H stretching at approximately 3000 cm^{-1}. C-H bending peaks were observed at 1420 and 1370 cm^{-1}.

Further observation of the spectra showed that the primary C=O peak of the neat CA membrane was located at 1733 cm^{-1}. For the plasticized membranes, these peaks shifted to 1734–1735 cm^{-1}. The shifted peaks indicated that citric acid and succinonitrile plasticizers were successfully incorporated into certain areas of the membrane. Increasing the plasticizer content promoted separation among the CA polymer chains, thereby reducing intermolecular interactions and increasing the vibrational frequencies of the carbonyl groups.

Analysis on membrane morphology was performed using SEM to analyze the impact of citric acid and succinonitrile addition on the separation of CA polymer chains. Fig. 3 shows the surface and cross-sectional morphologies of the pristine and plasticized CA membranes. The visual appearances of all the CA membranes, which are all fully transparent, are presented in the inset. Compared to pristine CA, membranes containing citric acid (CAC6) and succinonitrile (CASN6) showed that pore formation occurred all over the surface and across the cross section. Membrane thickness are measured using ImageJ, showing thickness of 21.27, 28.64, and 59.21 μm for CA, CAC6, and CASN6 sample, respectively.

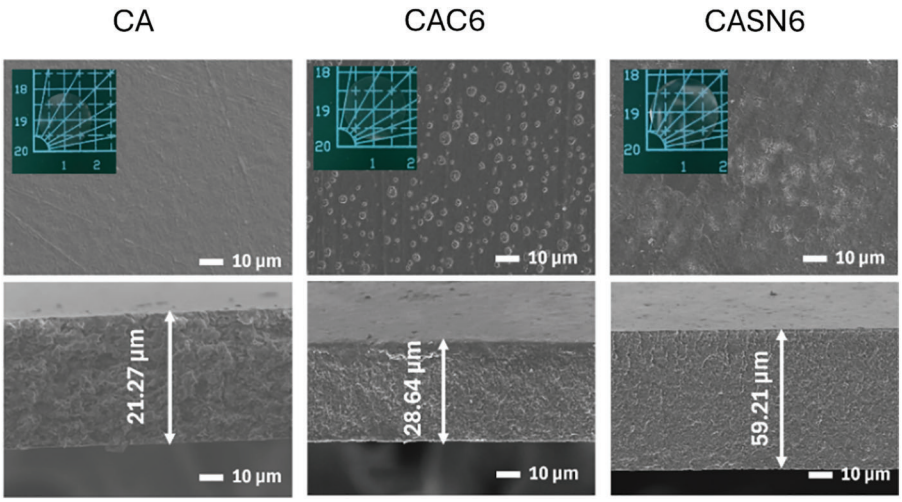

Figure 3: Surface (top row) and cross-section (bottom row) morphology of pristine and modified CA membrane

More detailed observations revealed smaller pores in the CASN6 membrane than those in the CAC6 membrane. This finding aligns with the FT-IR results (Fig. 2), where the CASN membrane showed an increase in the area ratio of the primary peak at wavenumber 1733 cm^{-1}, correlating with the weakening of the C=O bonds in the CA polymer chain [31,32].

A dimensional stability test was also performed to investigate the thermal shrinking behavior of the membranes by exposing CA and Celgard membranes to elevated temperatures from 30°C to 120°C. The results of the heat experiment are shown in Fig. 4. It can be seen that CA-based membrane showed negligible thermal deformation at high temperature while Celgard membrane experienced significant change in dimensionality.

This result indicates that the CA-based membrane can provide better dimensional stability and thermal resistance, thereby improving the safety of LIBs. Similar results were reported for cellulose membranes by Zhao with cellulose from cattail fibers and Liao with a hydroxyethyl cellulose composite [33,34].

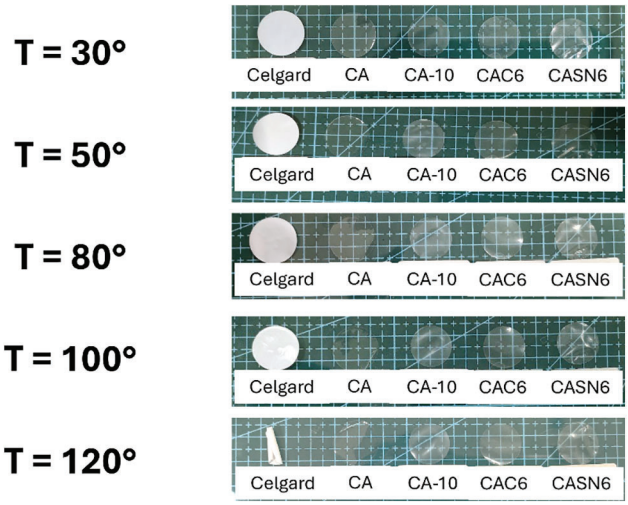

Figure 4: Photograph pictures of CA and Celgard membranes after heating from 30°C to 120°C

The XRD patterns of the pristine and modified CA are shown in Fig. 5. No diffraction peaks of the electrolyte salt, citric acid, and succinonitrile were found in any of the patterns, indicating that the salt and plasticizer were well dissolved in the CA matrix. All composites exhibited diffraction patterns similar to those of pristine CA, represented by strong peaks at approximately 18.7° and 13.2° and several weaker peaks. The addition of the electrolyte salt resulted in a stronger peak than that of neat CA. This implies an increase in the interplanar crystal spacing of the CA matrix, which may have occurred because of the insertion of large ClO_4^- anions into the CA lattice [35]. Furthermore, addition of citric acid and succinonitrile resulted in weaker and broader diffraction peaks. Additional diffraction humps were observed in the 25°–30° range. These observations suggest a rapid decrease in CA crystallinity resulting from coordination interactions between the added Li^+ and O atoms of CA. The plasticizers also promoted lower CA crystallinity, as indicated by the decreasing intensities of the characteristic peaks. The crystallinity index was calculated using the Segal method considering the characteristic CA peak at $2\theta = 18.7°$. The results are presented in Fig. 6, where it was observed that higher amounts of plasticizer resulted in a lower crystallinity index. These findings were consistent with the peak shifts in the FT-IR spectra, as previously explained [36].

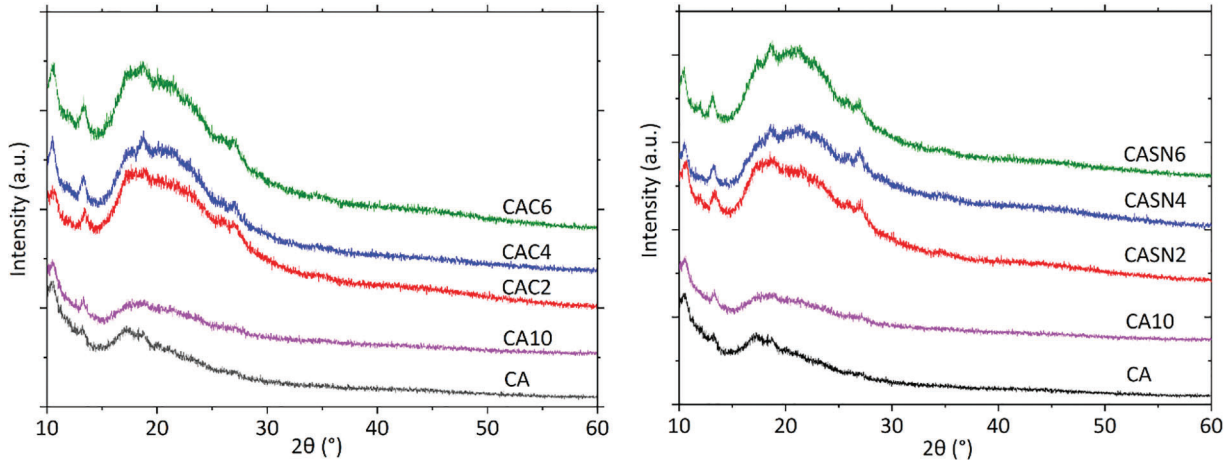

Figure 5: XRD patterns of pristine and modified CA membrane

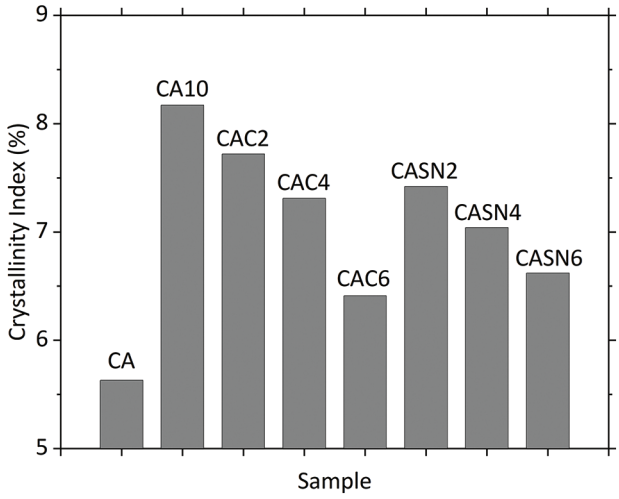

Figure 6: Crystallinity index of pristine and modified CA membranes

Differential scanning calorimetry (DSC) is widely used in academia and research to analyze the thermal properties of polymers. This enables the measurement of the glass transition temperature (T_g), melting temperature (T_m), and crystallization temperature (T_c) of polymers, polymer blends, and polymer composites. The glass transition temperature (T_g) of a polymer is widely acknowledged as a critical factor for assessing the compatibility of its components. A fully miscible polymer blend exhibits a single T_g, while an immiscible polymer blend displays multiple T_g values. Comparing the DSC thermograms of the pristine and modified CA membranes, it was found that all membranes only had a single T_g, indicating homogeneous blending of the polymer matrix, electrolyte salt, and plasticizer.

DSC thermograms of the pristine and modified CA membranes are presented in Fig. 7. Adding the electrolyte salt to the pristine CA membrane increased the T_g of the salt-doped CA membrane. However, the incorporation of plasticizers reduced the T_g. This indicated the successful plasticization of citric acid and succinonitrile in the CA membrane [37]. The broad endothermic peak between ambient temperature and 100°C denotes the water desorption of the polysaccharide [38]. This phenomenon is caused by the residual moisture or solvents with low boiling points.

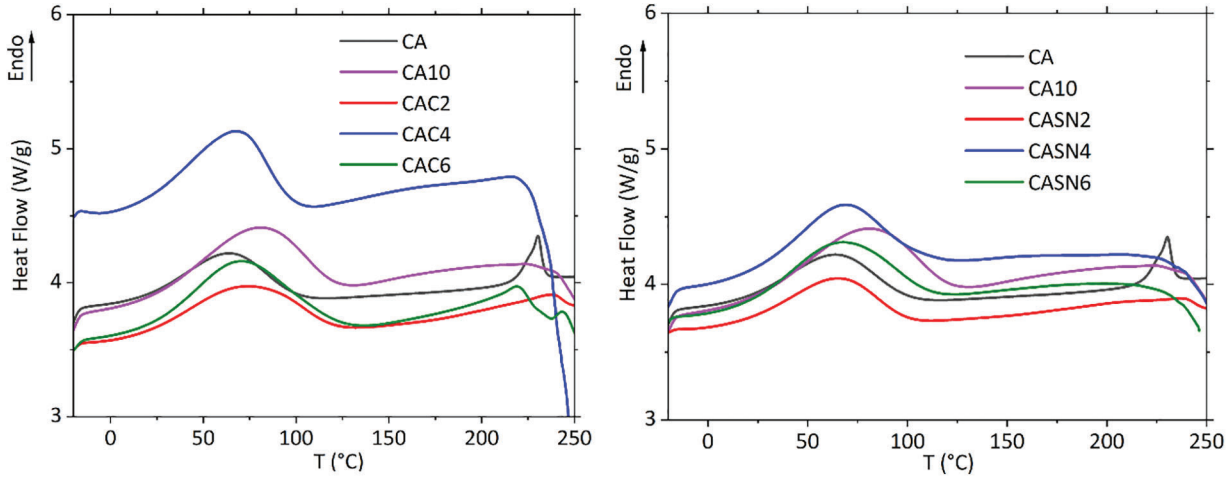

Figure 7: DSC thermogram of pristine and modified CA membrane

The thermal stabilities of the pristine and modified CA membranes were assessed using thermogravimetric analysis (TGA). Table 2 lists the detailed decomposition temperatures and specific weight loss percentages across the temperature ranges. The TGA profiles of these membranes are shown in Fig. 8. Onset temperature was determined according to ISO 11358-1 concerning the Thermogravimetry (TG) of Polymers, which defined it as the point of intersection of the starting-mass baseline and the tangent to the TGA curve at the point of maximum gradient. The incorporation of electrolyte salt improved the membrane onset decomposition temperature from 142.36°C to 285.73°C as seen from Fig. 8a. This behavior indicates that the $LiClO_4$ salt particles were well dispersed in the CA matrix [39]. The increase in the thermal stability of the CA/$LiClO_4$ composite is influenced by the contact of the CA membrane with the salt particles. These particles cover the membrane and fill its pores, thereby acting as a physical barrier against the transport of volatile decomposition products from the CA matrix. This certainly helps delay the thermal degradation of the CA membrane [40,41]. In addition to the improved onset decomposition temperature, the weight loss percentage also increased. Similar behavior was also observed for samples CAC-0 and CASN-0 in Fig. 8b, in which the addition of citric acid and succinonitrile plasticizer also enhanced the membrane thermal stability, as indicated by the increasing onset Td from 142.36°C to 281.86°C and 314.79°C, respectively.

Table 2: Decomposition temperature and weight loss percentages

Sample	Onset T_d, °C	T10%, °C	T25%, °C	T75%, °C	Residue after 450°C
Pristine CA	142.36	135.03	188.71	350.94	10.84%
CA10	285.73	168.49	293.98	347.58	17.24%
CAC0	310.81	219.91	352.88	385.83	12.86%
CAC2	281.86	293.67	339.92	380.68	14.47%
CAC4	252.13	223.83	283.20	371.86	16.49%
CAC6	248.15	168.96	261.05	362.00	18.39%
CASN0	321.98	227.39	355.59	387.36	12.66%
CASN2	314.79	298.65	342.63	379.96	13.73%
CASN4	272.85	155.09	277.90	333.74	17.04%
CASN6	262.69	141.53	268.28	335.77	18.37%

A further increase in the plasticizer concentration resulted in a lower onset T_d value, which was caused by the increasing crosslinking effect and, therefore, enhanced separation between the CA polymer chains. Similar results were obtained for T10%, T25%, and T75%. The optimum plasticizing effect on the thermal stability of the modified CA membranes was 2% [42].

The electrochemical performance of the pristine and modified CA membranes was evaluated using a complex impedance plot at room temperature, as shown in Fig. 9. The Nyquist plot, comprising the real impedance (Z′) and imaginary impedance (Z″) axes, involves a high-frequency semicircle representing the bulk capacitance and a low-frequency spike representing the bulk resistance of the sample. This is caused by bulk ion migration and the difference in ion relaxation times. The nonexistent semicircle indicates the presence of a resistive component in the polymer electrolyte. The imperfect electrode-electrolyte interface resulted in an inclined spike angle. The bulk resistance was calculated from the intercept of the real impedance axis between the semicircle and the spike.

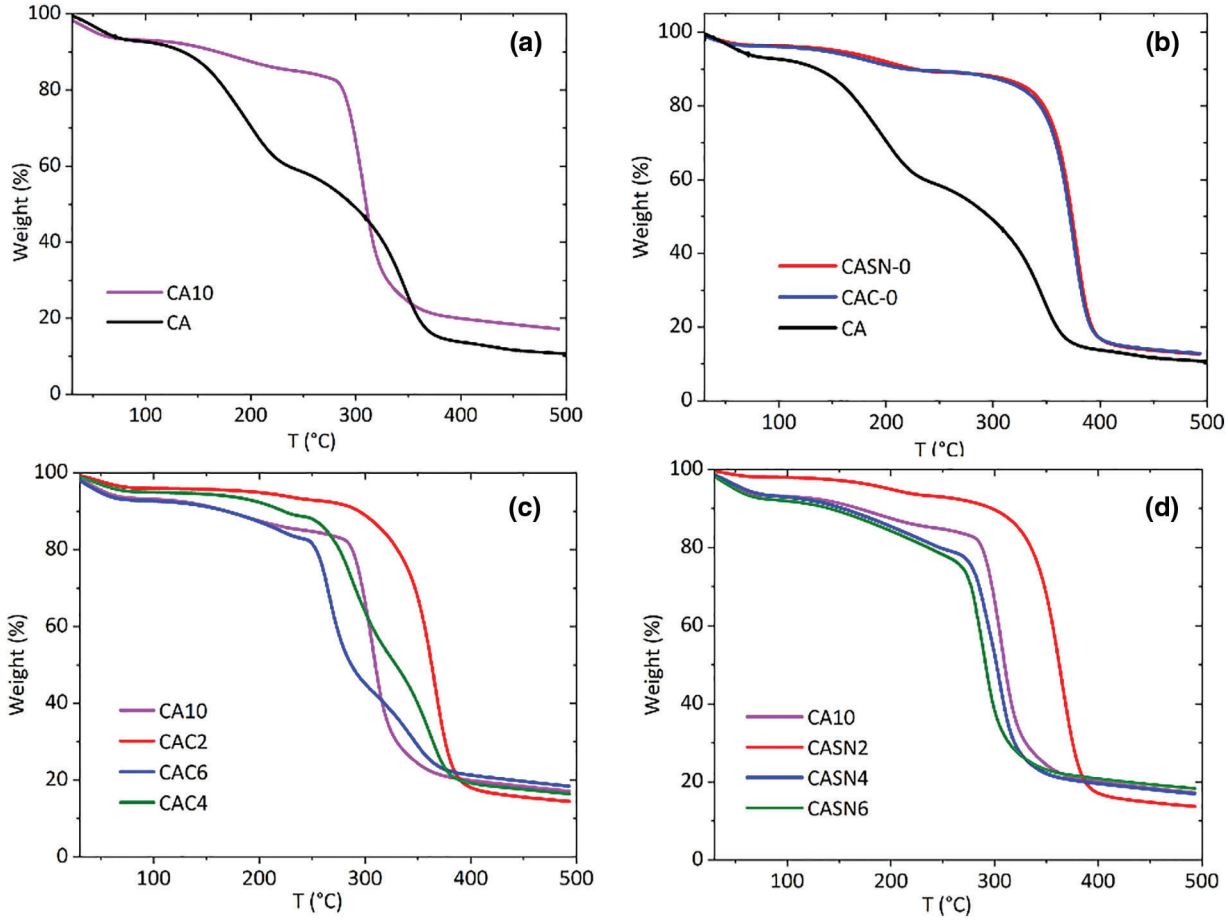

Figure 8: TGA curve of (a) pristine *vs*. salt-doped CA membrane; (b) pristine *vs*. plasticized CA membrane; and CA membrane plasticized using (c) citric acid and (d) succinonitrile

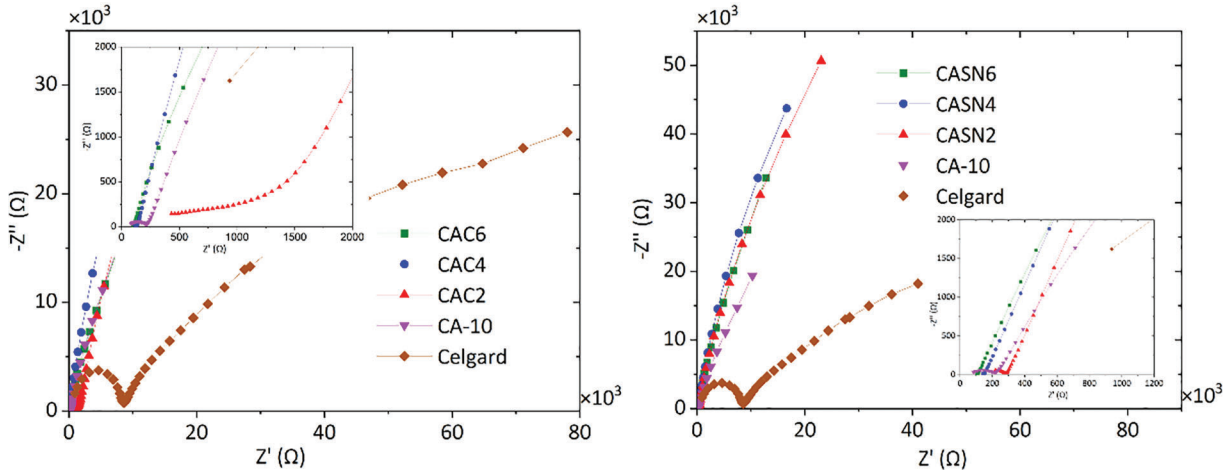

Figure 9: Nyquist plot of CA and Celgard membrane

The CA membrane doped with $LiClO_4$ salt (sample CA-10) showed an ionic conductivity value of 4.69 × 10^{-6} S/cm. Addition of citric acid and succinonitrile has improved the ionic conductivity of CA membrane from 4.69 × 10^{-6} S/cm to 1.27 × 10^{-5} and 2.73 × 10^{-5} S/cm, respectively. An obvious enhancement was also observed in the ionic conductivity compared with the commercially available Celgard separator, that is, 2.14 × 10^{-7} S/cm. The higher ionic conductivity of the plasticized CA membrane might be due to the more amorphous nature of the polymer matrix and lower glass transition temperature, as seen in the DSC measurements.

This work proposes a CA-based membrane plasticized by citric acid and succinonitrile as a renewable material to substitute commercial polyolefin membranes as separators in LIBs. Citric acid plasticizer was also involved in the carboxymethylcellulose-$LiClO_4$ complex, resulting in an ionic conductivity of 1.24 × 10^{-7} S/cm [43]. The cellulose acetate membrane plasticized with 25 wt. % PEG-600 improved Mg $(CF_3SO_3)^2$-doped membrane to 3.76 × 10^{-4} S/cm [44]. In most instances, a high amount of plasticizer is required to exert a significant effect on polymer electrolyte complexes. This could have a negative impact on thermal stability, which is a non-negotiable property for an LIBs component. Work by Samsi involved 50 wt. % ethylene carbonate to improve CA-based membrane ionic conductivity [45]. Another work by Harun presented a CA membrane doped with ammonium tetrafluoroborate with 30% PEG addition, resulting in 1.41 × 10^{-5} S/cm [46]. The oligo-PEG–LiI complex required 32.4 wt. % citric acid to achieve conductivity value of 5.43 × 10^{-5} S/cm [47]. In this study, a maximum of only 6 wt. % amount of citric acid and succinonitrile was incorporated to give similar performance.

Proper electrochemical stability is an important criterion for an energy storage device to maintain safety performance and to ensure that the electrolyte can withstand repetitive charging and discharging processes. The electrochemical stability window (ESW) value was identified as a potential limit by linear sweep voltammetry (LSV) measurements. LSV voltammogram is presented on Fig. 10. It was found that the ESW of these membranes are 3.19 and 3.43 V for CAC6 and CASN6 membrane, respectively. A sharp rise on the current after the breakdown point indicates the onset of the oxidation process of the electrolyte. These values are higher compared to unplasticized CA membrane in which the LSV was measured at 3.03 V [30] and 2.98 V [44].

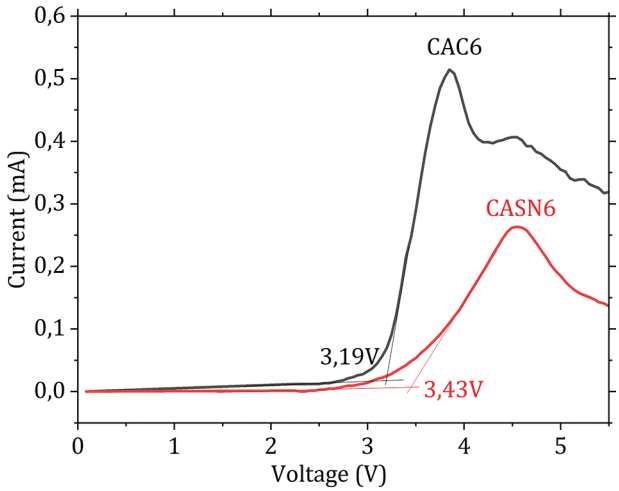

Figure 10: LSV voltammogram of CAC6 and CASN6 membrane

The frequency-dependent AC conductance spectra of the pristine and modified CA membranes are shown in Fig. 11. In this figure, we can observe conductance spectra consisting of a low-frequency

dispersion caused by the electrode polarization effect and a frequency-independent plateau region caused by frequency-independent conductivity.

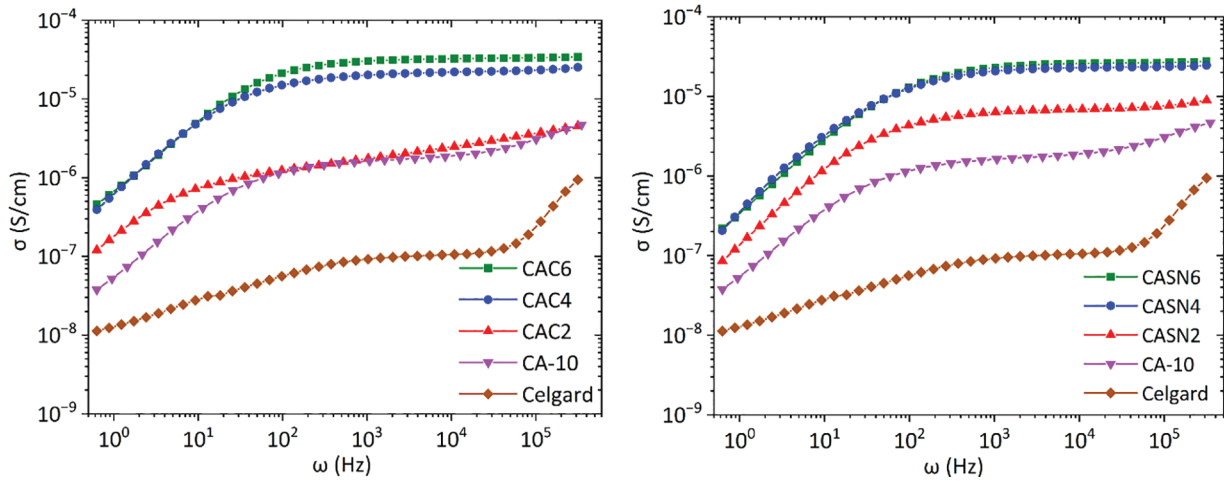

Figure 11: Conductivity spectra of CA and Celgard membrane

A deeper understanding of the conductivity and polarization across the electrode/electrolyte interface can be obtained from dielectric properties. The complex dielectric permittivity equation is $\varepsilon^* = \varepsilon' + j\varepsilon''$, where ε' is the real permittivity (dielectric constant), and ε' is the imaginary permittivity (dielectric loss). ε'' can be defined as $\sigma/(\omega.\varepsilon_0)$, where ω is the angular frequency and ε_0 is the free-space permittivity. The mathematical expressions for ε' and ε'' can then be defined using Eqs. (2) and (3):

$$\varepsilon' = \frac{Z''}{\omega C_0 \left(Z'^2 + Z''^2\right)} \tag{2}$$

$$\varepsilon'' = \frac{Z'}{\omega C_0 \left(Z'^2 + Z''^2\right)} \tag{3}$$

Fig. 12 (top row) shows frequency-dependent loss tangent (tan δ) plots for the CA membranes and commercial Celgard. Based on these measurements, both pristine and modified CA membranes consistently showed superior dielectric constants compared to those of commercial Celgard membranes. As more plasticizers were added, there were apparent shifts in the relaxation peaks towards the higher-frequency region. These shifts and increases in tangent loss are caused by the higher number of available charge carriers responsible for ionic conduction [48].

The dielectric constant as a function of frequency among the different CA membranes and Celgard can is shown in Fig. 12 (bottom row). The low-frequency region reveals the dispersion of permittivity in these samples. The highest dielectric constants were obtained for the CAC6 and CASN6 samples. A lower amount of plasticizer resulted in a lower dielectric constant. In accordance with the conductivity data, the pristine and modified CA membranes had higher dielectric constants than the Celgard membrane. Membranes with a high dielectric constant help free up ionic charge species inside the polymer electrolyte membrane. At low frequencies, plasticizers are present in more localized ionic species within the system, resulting in a high dielectric constant. Increasing the frequency affected the electrical relaxation process, where the dielectric constant values decreased for all specimens. Electrical dipoles are becoming increasingly difficult to orient and reorient themselves [49].

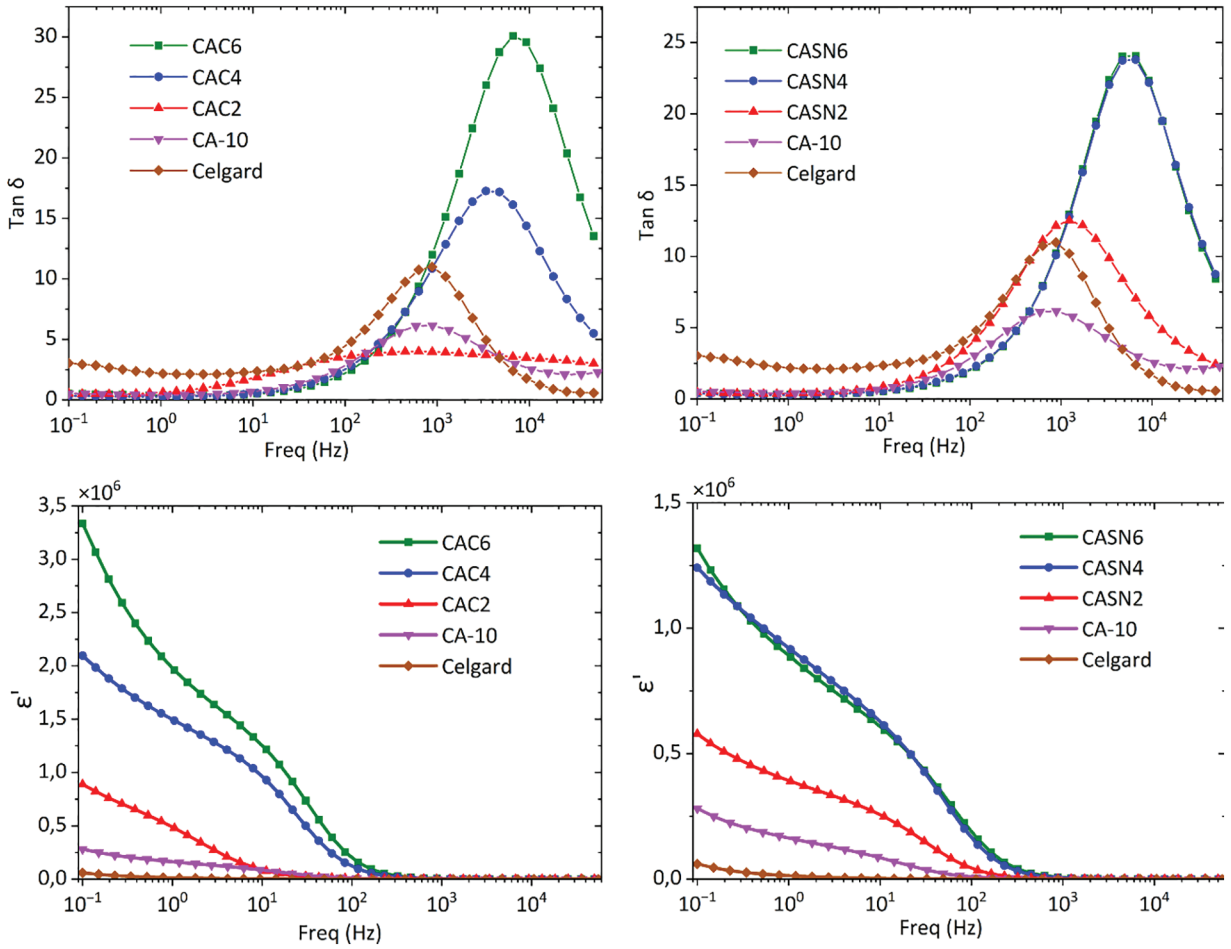

Figure 12: Loss tangent (top row) and dielectric constant (bottom row) of CA and Celgard membrane

4 Conclusion

Cellulose-acetate-based solid polymer electrolyte membranes plasticized with citric acid and succinonitrile were successfully fabricated using a solution casting method. The interactions between the plasticizers, polymer hosts, and electrolyte salts were studied using FT-IR spectroscopy. The XRD results demonstrated that a higher amount of plasticizer increased the amorphousness of CPE, which in turn enhanced ion transport and increased ionic conductivity. The maximum ionic conductivity was 2.73×10^{-5} S/cm with a 6% succinonitrile acid plasticizer. The dielectric properties indicated charge carrier availability owing to the plasticizing effect and ionic conduction in the membrane. These results demonstrate that the valorization of sustainable materials has a promising future as a substitute for fossil-based products currently used in lithium-ion battery applications.

Acknowledgement: The authors would like to thank the Integrated Laboratory of Advanced Materials Characterization, National Research and Innovation Agency of Indonesia (BRIN), and the Integrated Laboratory and Research Center, Universitas Indonesia, for the material characterization facility.

Funding Statement: This work was financially supported by the Indonesia Endowment Fund for Education (LPDP) scholarship, funded by the Ministry of Finance, Republic of Indonesia (award number 202112210108100).

Author Contributions: The authors confirm contribution to the paper as follows: study conception and design: Christin Rina Ratri, Adam Febriyanto Nugraha; data collection: Christin Rina Ratri, Qolby Sabrina; analysis and interpretation of results: Christin Rina Ratri, Sotya Astutiningsih, Mochamad Chalid; draft manuscript preparation: Christin Rina Ratri, Adam Febriyanto Nugraha. All authors reviewed the results and approved the final version of the manuscript.

Availability of Data and Materials: Data is available on request from the authors.

Ethics Approval: Not required.

Conflicts of Interest: The authors declare that they have no conflicts of interest to report regarding the present study.

References

1. Sun Z, Wang Z, Tian Y, Wang G, Wang W, Yang M, et al. Progress, outlook, and challenges in lead-free energy-storage ferroelectrics. Adv Electron Mater. 2020;6(1):1–34. doi:10.1002/aelm.201900698.
2. Costa CM, Lee YH, Kim JH, Lee SY, Lanceros-Méndez S. Recent advances on separator membranes for lithium-ion battery applications: from porous membranes to solid electrolytes. Energy Storage Mater. 2019;22:346–75. doi:10.1016/j.ensm.2019.07.024.
3. Sun Z, Zhao S, Wang T, Jing H, Guo Q, Gao R, et al. Achieving high overall energy storage performance of KNN-based transparent ceramics by ingenious multiscale designing. J Mater Chem A. 2024;12(27):16735–47. doi:10.1039/d4ta02425g.
4. Ghiji M, Novozhilov V, Moinuddin K, Joseph P, Burch I, Suendermann B, et al. A review of lithium-ion battery fire suppression. Energies. 2020;13(19):1–30. doi:10.3390/en13195117.
5. Bhute MV, Kondawar SB. Electrospun poly (vinylidene fluoride)/cellulose acetate/$AgTiO_2$ nanofibers polymer electrolyte membrane for lithium ion battery. Solid State Ion. 2019;333:38–44. doi:10.1016/j.ssi.2019.01.019.
6. Wang J, Wang C, Wang W, Li W, Lou J. Carboxymethylated nanocellulose-based gel polymer electrolyte with a high lithium ion transfer number for flexible lithium-ion batteries application. Chem Eng J. 2022;428:132604. doi:10.1016/j.cej.2021.132604.
7. Chen R, Liu F, Chen Y, Ye Y, Huang Y, Wu F, et al. An investigation of functionalized electrolyte using succinonitrile additive for high voltage lithium-ion batteries. J Power Sources. 2016;306:70–7. doi:10.1016/j.jpowsour.2015.10.105.
8. Zalosh R, Gandhi P, Barowy A. Lithium-ion energy storage battery explosion incidents. J Loss Prev Process Ind. 2021;72:104560. doi:10.1016/j.jlp.2021.104560.
9. Jiang F, Yin L, Yu Q, Zhong C, Zhang J. Bacterial cellulose nanofibrous membrane as thermal stable separator for lithium-ion batteries. J Power Sources. 2015;279:21–7. doi:10.1016/j.jpowsour.2014.12.090.
10. Pereira DJ, McRay HA, Bopte SS, Jalilvand G. H_2O/HF scavenging mechanism in cellulose-based separators for lithium-ion batteries with enhanced cycle life. ACS Appl Mater Interfaces. 2024;16(5):5745–57. doi:10.1021/acsami.3c14558.
11. Zhang J, Liu Z, Kong Q, Zhang C, Pang S, Yue L, et al. Renewable and superior thermal-resistant cellulose-based composite nonwoven as lithium-ion battery separator. ACS Appl Mater Interfaces. 2013;5(1):128–34. doi:10.1021/am302290n.
12. Hu J, Liu Y, Zhang M, He J, Ni P. A separator based on cross-linked nano-SiO_2 and cellulose acetate for lithium-ion batteries. Electrochim Acta. 2020;334:135585. doi:10.1016/j.electacta.2019.135585.
13. Lizundia E, Costa CM, Alves R, Lanceros-Méndez S. Cellulose and its derivatives for lithium ion battery separators: a review on the processing methods and properties. Carbohydr Polym Technol Appl. 2020;1:100001. doi:10.1016/j.carpta.2020.100001.
14. Arundati AH, Ratri CR, Chalid M, Aqoma H, Nugraha AF. A combination of nonsolvent and thermally induced phase separation (N-TIPS) technique for the preparation of highly porous cellulose acetate membrane as lithium-ion battery separators. Ionics. 2023;123456789. doi:10.1007/s11581-023-05276-5.

15. Vidal R, Alberola-Borràs JA, Habisreutinger SN, Gimeno-Molina JL, Moore DT, Schloemer TH, et al. Assessing health and environmental impacts of solvents for producing perovskite solar cells. Nat Sustain. 2021;4(3):277–85. doi:10.1038/s41893-020-00645-8.
16. Daniels PH. A brief overview of theories of PVC plasticization and methods used to evaluate PVC-plasticizer interaction. J Vinyl Addit Technol. 2009;15(4):219–23. doi:10.1002/vnl.20211.
17. Bonifacio A, Bonetti L, Piantanida E, De Nardo L. Plasticizer design strategies enabling advanced applications of cellulose acetate. Eur Polym J. 2023;197:112360. doi:10.1016/j.eurpolymj.2023.112360.
18. Gupta S, Varshney PK. Effect of plasticizer concentration on structural and electrical properties of hydroxyethyl cellulose (HEC)-based polymer electrolyte. Ionics. 2017;23(6):1613–7. doi:10.1007/s11581-017-2116-8.
19. Mustafa MF, Ridwan NIM, Hatta FF, Yahya MZA. Effect of dimethyl carbonate plasticizer on ionic conductivity of methyl cellulose-based polymer electrolytes. Malaysian J Anal Sci. 2012;16(3):283–9.
20. Rizzuto C, Teeters DC, Barberi RC, Castriota M. Plasticizers and salt concentrations effects on polymer gel electrolytes based on poly (methyl methacrylate) for electrochemical applications. Gels. 2022;8(6):363. doi:10.3390/gels8060363.
21. Lammens TM, Le Nôtre J, Franssen MCR, Scott EL, Sanders JPM. Synthesis of biobased succinonitrile from glutamic acid and glutamine. ChemSusChem. 2011;4(6):785–91. doi:10.1002/cssc.201100030.
22. Alarco PJ, Abu-Lebdeh Y, Abouimrane A, Armand M. The plastic-crystalline phase of succinonitrile as a universal matrix for solid-state ionic conductors. Nat Mater. 2004;3(7):476–81. doi:10.1038/nmat1158.
23. MacFarlane DR, Forsyth M. Plastic crystal electrolyte materials: new perspectives on solid state ionics. Adv Mater. 2001;13(12–13):957–66. doi:10.1002/1521-4095(200107).
24. Lv P, Li Y, Wu Y, Liu G, Liu H, Li S, et al. Robust succinonitrile-based gel polymer electrolyte for lithium-ion batteries withstanding mechanical folding and high temperature. ACS Appl Mater Interfaces. 2018;10(30):25384–92. doi:10.1021/acsami.8b06800.
25. Zhang Q, Liu K, Ding F, Li W, Liu X, Zhang J. Safety-reinforced succinonitrile-based electrolyte with interfacial stability for high-performance Lithium batteries. ACS Appl Mater Interfaces. 2017;9(35):29820–8. doi:10.1021/acsami.7b09119.
26. Kim GY, Petibon R, Dahn JR. Effects of succinonitrile (SN) as an electrolyte additive on the impedance of $LiCoO_2$/graphite pouch cells during cycling. J Electrochem Soc. 2014;161(4):506–12. doi:10.1149/2.014404jes.
27. Wang J, Yang J, Shen L, Guo Q, He H, Yao X. Synergistic effects of plasticizer and 3D framework towards high-performance solid polymer electrolyte for room-temperature solid-state lithium batteries. ACS Appl Energy Mater. 2021;4(4):4129–37. doi:10.1021/acsaem.1c00468.
28. Max B, Salgado JM, Rodriguez N, Cortes S, Converti A, Dominguez JM. Biotechnological productions of citric acid. Braz J Microbiol. 2010;41:862–75. doi:10.1590/S1517-83822010000400005.
29. Nasution H, Harahap H, Dalimunthe NF, Ginting MHS, Jaafar M, Tan OOH, et al. Hydrogel and effects of crosslinking agent on cellulose-based hydrogels: a review. Gels. 2022;8(9):568. doi:10.3390/gels8090568.
30. Bhuvaneswari B, Sivabharathy M, Prasad LG, Selvasekarapandian S. Structural, thermal and electrochemical characterization of cellulose acetate-based solid biopolymer electrolyte for zinc ion batteries. Ionics. 2022;28(8):3865–75. doi:10.1007/s11581-022-04616-1.
31. Lee C, Kang SW. Influence of citric acid concentrations on the porosity and performance of cellulose acetate-based porous membranes: a comprehensive study. Int J Biol Macromol. 2024;263:130243. doi:10.1016/j.ijbiomac.2024.130243.
32. Zheng G, Zeng Z, Chen Y, Wang X, Sun D, Cui C. Versatile electrospinning technology on solid-state electrolytes for energy storage: a brief review. J Energy Storage. 2024;86:111285. doi:10.1016/j.est.2024.111285.
33. Zhao X, Wang W, Huang C, Luo L, Deng Z, Guo W, et al. A novel cellulose membrane from cattail fibers as separator for Li-ion batteries. Cellulose. 2021;28(14):9309–21. doi:10.1007/s10570-021-04110-3.
34. Liao H, Zhang H, Hong H, Li Z, Qin G, Zhu H, et al. Novel cellulose aerogel coated on polypropylene separators as gel polymer electrolyte with high ionic conductivity for lithium-ion batteries. J Memb Sci. 2016;514:332–9. doi:10.1016/j.memsci.2016.05.009.

35. Wu XL, Xin S, Seo HH, Kim J, Guo YG, Lee JS. Enhanced Li^+ conductivity in PEO-LiBOB polymer electrolytes by using succinonitrile as a plasticizer. Solid State Ion. 2011 Mar;186(1):1–6. doi:10.1016/j.ssi.2011.01.010.
36. Jeedi VR, Ganta KK, Mallaiah Y, Swarnalatha R, Reddy SN, Chary AS. Influence of succinonitrile plasticizer on ionic conductivity, structural and dielectric properties of potassium-based PEO/PVdF blend polymer electrolyte. J Polym Res. 2022;29(2):64. doi:10.1007/s10965-022-02912-y.
37. Fridman OA, Sorokina AV. Criteria of efficiency of cellulose acetate plasticization. Polym Sci-Ser B. 2006;48(5):233–6. doi:10.1134/S1560090406090028.
38. Barud HS, de Araújo Júnior AM, Santos DB, de Assunção RMN, Meireles CS, Cerqueira DA, et al. Thermal behavior of cellulose acetate produced from homogeneous acetylation of bacterial cellulose. Thermochim Acta. 2008;471(1–2):61–9. doi:10.1016/j.tca.2008.02.009.
39. Vaggar GB, Sirimani VB, Sataraddi DP, Hiremath NM, Bhajantri F. Effect of filler materials on thermal properties of polymer composite materials: a review. Int J Eng Res Technol. 2021;10(8):1–5.
40. Mat Yazik MH, Sultan MTH, Jawaid M, Abu Talib AR, Mazlan N, Md Shah AU, et al. Effect of nanofiller content on dynamic mechanical and thermal properties of multi-walled carbon nanotube and montmorillonite nanoclay filler hybrid shape memory epoxy composites. Polymers. 2021;13(5):1–21. doi:10.3390/polym13050700.
41. Yuanita E, Nugraha AF, Jumahat A, Mochtar MA, Chalid M. Extraction of cellulose from arenga pinnata "ijuk" fiber for polypropylene composite: effect of multistage chemical treatment on the crystallinity and thermal behaviour of composite. South Afr J Chem Eng. 2024;48:112–20. doi:10.1016/j.sajce.2024.01.010.
42. Maizatul N, Norazowa I, Yunus WMZW, Khalina A, Khalisanni K. FTIR and TGA analysis of biodegradable poly (lactic acid)/treated kenaf bast fibre: effect of plasticizers. Pertanika J Sci Technol. 2013;21(1):151–60.
43. Maddu A, Sulaeman AS, Tri Wahyudi S, Rifai A. Enhancing ionic conductivity of carboxymethyl cellulose-lithium perchlorate with crosslinked citric acid as solid polymer electrolytes for lithium polymer batteries. Int J Renew Energy Dev. 2022;11(4):1002–11. doi:10.14710/ijred.2022.40090.
44. Gopinath G, Shanmugaraj P, Sasikumar M, Shadap M, Banu A, Ayyasamy S. Cellulose acetate-based magnesium ion conducting plasticized polymer membranes for EDLC application: advancement in biopolymer energy storage devices. Appl Surf Sci Adv. 2023;18:100498. doi:10.1016/j.apsadv.2023.100498.
45. Samsi NS, Zakaria R, Hassan OH, Azhan Yahya MZ, Ali AMM. X-ray diffraction and infrared studies on plasticized cellulose acetate complexed with ammonium iodide for solid polymer electrolyte. Mater Sci Forum. 2016;846:523–7. doi:10.4028/www.scientific.net/MSF.846.523.
46. Harun NI, Ali RM, Ali AMM, Yahya MZA. Dielectric behaviour of cellulose acetate-based polymer electrolytes. Ionics. 2012;18(6):599–606. doi:10.1007/s11581-011-0653-0.
47. Liang G, Xu W, Xu J, Shen X, Yao M. Influence of weight ratio of citric acid cross linker on the structure and conductivity of the crosslinked polymer electrolytes. Adv Mater Res. 2012;391–392:1075–9. doi:10.4028/www.scientific.net/AMR.391-392.1075.
48. Koduru HK, Bruno L, Marinov YG, Hadjichristov GB, Scaramuzza N. Mechanical and sodium ion conductivity properties of graphene oxide-incorporated nanocomposite polymer electrolyte membranes. J Solid State Electrochem. 2019;23(9):2707–22. doi:10.1007/s10008-019-04359-6.
49. Maheshwaran C, Kanchan DK, Mishra K, Kumar D, Gohel K. Flexible magnesium-ion conducting polymer electrolyte membranes: mechanical, structural, thermal, and electrochemical impedance spectroscopic properties. J Mater Sci Mater Electron. 2020;31(18):15013–27. doi:10.1007/s10854-020-04065-4.